



# Estimating Soil Thermal Conductivity by Weighted Average Models with Soil Solids as a Continuous Medium

V. R. Tarnawski<sup>1</sup> · W. H. Leong<sup>2</sup> · M. McCombie<sup>1</sup> · G. Bovesecchi<sup>3</sup>

Received: 7 August 2022 / Accepted: 3 October 2022  
© The Author(s) 2022

## Abstract

In an attempt to further simplify and to refine the modeling of soil thermal conductivity ( $\lambda$ ), two novel weighted average models (WAMs) were developed in which soil solids represent the continuous phase. In the first model, WAM<sub>s</sub>-1, the continuous phase consists of two distinctive minerals groups (quartz and compounded remaining soil minerals), while air and water are treated as dispersed components. In the second model, WAM<sub>s</sub>-2, all soil minerals are compounded and considered the continuous phase, while air and water are dispersed components. In contrast to de Vries' original WAM with two continuous phases (soil air or soil water), the proposed models are very simple due to the following assumptions: using soil solids as a single continuous medium lead to eliminating the discontinuity of thermal conductivity when switching between soil air and soil water as continuous medium, and using the thermal conductivity of dry air simplifies a complex expression for an apparent thermal conductivity of humid soil air. Both models were successfully calibrated and validated using 39 Canadian Field Soil database and 3 Standard Sands and were successfully applied to 10 Chinese soils.

**Keywords** Canadian soils · Chinese soils · Modeling · Soil solids as continuous phase · Standard sands · Thermal conductivity

## List of Symbols

### Latin

$g$  Control factor  
 $m$  Mass fraction

---

✉ G. Bovesecchi  
gianluigi.bovesecchi@uniroma2.it

<sup>1</sup> Division of Engineering, Saint Mary's University, Halifax, Canada

<sup>2</sup> Department of Mechanical and Industrial Engineering, Toronto Metropolitan University, Toronto, Canada

<sup>3</sup> Department of Enterprise Engineering, University of Rome "Tor Vergata", Rome, Italy

$M$	Number of model fitted coefficients
$n$	Porosity
$N$	Number of measurements
$S_r$	Degree of saturation
$T$	Temperature [ $^{\circ}\text{C}$ ] or [ $\text{K}$ ]

### Greek

$\theta$	Volumetric fraction (quartz, other minerals, water, air)
$\Theta$	Volumetric content applied to soil solids (quartz, other minerals)
$\kappa$	Soil component weighting factor
$\lambda$	Thermal conductivity [ $\text{W}\cdot\text{m}^{-1}\cdot\text{K}^{-1}$ ]
$\rho$	Density [ $\text{kg}\cdot\text{m}^{-3}$ ]

### Subscripts

a	Air
a-app	Humid soil air
cal	Calcite
cl	Clay
cr	Critical
dol	Dolomite
dry	Dryness
ECM	Electrical conductivity model
est	Estimated
exp	Experimental
i	Generic component
o-min	Other minerals (except quartz)
qtz	Quartz
s	Soil solids
sa	Sand
sat	Saturation
si	Silt
v	Water vapor
w	Water

### Abbreviations

AB	Alberta soil
BC	British Columbia soil
MN	Manitoba soil
NB	New Brunswick soil
NS	Nova Scotia soil
ON	Ontario soil
PE	Prince Edward Island soil
QC	Quebec soil
$SD$	Standard deviation
SK	Saskatchewan soil
WAM	Weighted average model

## 1 Introduction

A thorough knowledge of the soil's thermal conductivity ( $\lambda$ ) is essential for the design of earth-contact installations, such as high-voltage power cables, ground heat exchangers, vaults containing nuclear waste, and steam and hot water pipelines. Reliable data on the thermal conductivity of the soil are also necessary for assessing the long-term impact of underground facilities on the earth surface environment. Despite this, it is rare to find trustworthy and complete thermal conductivity data, covering a full range of the degree of saturation ( $S_r$ ). This is due to the great diversity of soil texture, the unusual shape of soil particles, the soil water redistribution, and the labor-intensive measurement procedures that require unique and expensive equipment [1, 2]. In addition, thermal conductivity measurements are prone to error because the operating principle of thermal conductivity probes is based on the classical theory of conduction heat flow in solids. Extending this theory to porous soil systems raises several problems [3, 4] such as a complex and porous capillary system, contact resistance between the thermal conductivity probe and surrounding soil particles, and a simultaneous heat and soil moisture flow in combination with latent heat effects. Consequently, soil thermal conductivity measurements are prone to errors that are difficult to assess. For this reason, estimating soil thermal conductivity from general soil properties has attracted increasing attention. Several thermal conductivity models have been developed in the past [5–20]. Of these, six are based on semi-physical principles [6, 9, 10, 14, 16, 20], one is based on a statistical-physical principle [11] and the remaining eight are based on empirical principles [5, 7, 8, 12, 13, 15, 17, 19]. For more details on the previous thermal conductivity models see [21]. In general, the physical-based (mechanistic) models use a simplified theory of conduction heat flow in solids adapted to porous media. Consequently, they have added value in estimating thermal conductivity and extrapolation capability when applied to different soil textures. These models usually take into account the main characteristics of the soil system, such as porosity ( $n$ ), density of solids ( $\rho_s$ ), mineral composition, texture, water content,  $\lambda$  of water ( $\lambda_w$ ), air ( $\lambda_a$ ), and solids ( $\lambda_s$ ) as well as some discrete parameters that cannot be observed directly (e.g., thermal conductivity of water vapor with latent heat effects,  $\lambda_v$ ). The thermal conductivity of solids ( $\lambda_s$ ) is also commonly used in the majority of models. However, due to the often-unknown mineralogy of the soils, it is very difficult to assess representative values of  $\lambda_s$ . For this reason,  $\lambda_s$  is usually treated as a fitting parameter. Therefore, complete soil mineralogy data are essential for the successful development and verification of thermal conductivity models. Tarnawski et al. [20] reviewed and analyzed de Vries' model [6] using a complete thermal conductivity database of 39 Canadian Field Soils and 3 Standard Sands; each soil thermal conductivity data set was measured using the transient thermal probe technique at room temperature ( $T$ ). In general, the de Vries model (deV-1) provides good estimation ( $\lambda_{est}$ ) for fine and coarse textured soils. However, the wide application of this model is considerably limited by its considerable complexity and the obligatory use of numerous coefficients that are very difficult to determine. Originally, these

coefficients were obtained from fitting to selected soil thermal conductivity data that may not be fully applicable to different field soils. As a result, these coefficients are often roughly estimated or taken from other published data. Furthermore, deV-1 is based on several unrealistic assumptions regarding soil structure: solid grains are considered as rotated oblate ellipsoids, all grains are identical in size, do not touch each other, and are uniformly dispersed in a homogeneous continuous medium (air or water). In fact, deV-1 uses two distinctly different continuous media (*water* or *air*:  $\lambda_w/\lambda_a \approx 25$ ) with a boundary point (at the critical soil water content,  $\theta_{cr}$ ) between them. As a result, there is an obvious step change in the calculated thermal conductivity (at  $\theta_{cr}$ ) which has no physical interpretation. Furthermore, there are no clear guidelines for  $\theta_{cr}$  values when applied to different soil textures. Additionally, the use of deV-1 between dryness and  $\theta_{cr}$  was not recommended and an alternative linear interpolation of thermal conductivity was recommended. For soils at elevated temperatures (30–90 °C), deV-1 obviously underestimates the experimental thermal conductivity. This issue was partially reduced by replacing the thermal conductivity of dry air with the thermal conductivity of moist air ( $\lambda_{app} = \lambda_a + \lambda_v$ ), where  $\lambda_v$  represents the thermal conductivity of migrating water vapor carrying the latent heat [6]. Even though only a satisfactory agreement with the measured thermal conductivity data was obtained, the above issues are very difficult to solve within the framework of the deV-1 model, so the development of a new model is urgently needed. Perhaps, new research should consider a simplified, but still versatile, weighted average model for soils that includes only one physically based, continuous phase that is applicable to a full range of wetness. The new model should be far simpler to use compared to the deV-1 model, while still maintaining close  $\lambda_{est}$  to  $\lambda_{exp}$ .

The main objective of this paper is therefore to develop two weighted average models with soil solids (*s*) as the continuous medium (WAM<sub>s</sub>). The first model (WAM<sub>s</sub>-1) considers two distinctly different mineral groups (i.e., quartz and other minerals) as the continuous medium. Quartz is one of the most common minerals in the Earth's crust and its  $\lambda$  is superior (7.6 W·m<sup>-1</sup>·K<sup>-1</sup>) with respect to other minerals (2.2 W·m<sup>-1</sup>·K<sup>-1</sup>); therefore, quartz is treated separately from other minerals. In turn, the second model (WAM<sub>s</sub>-2) considers all soil minerals as consolidated and as a result forming the continuous medium. The fundamental principles of these two models originate from Maxwell's electrical conductivity model (ECM) [22], for non-interacting solid spheres immersed in the continuous medium, and its extension to identical elongated ellipsoids by Fricke [23]. In contrast to the ECM, its current adaptation to conduction heat flow in unsaturated soils assumes that the continuous medium is formed from mineral soil components while air and water are dispersed components. This modeling approach reflects the actual soil structure more realistically than in the deV-1, where soil solids are compacted together to naturally form the continuous phase. Both new models are subject to calibration and thorough verification by comparing their  $\lambda_{est}$  with measured thermal conductivity values of 39 Canadian Field Soils and 3 Standard Sands. Then their predicted thermal conductivity is compared to the  $\lambda_{est}$  obtained with the original deV-1 model [20].

## 2 Materials and Methods

### 2.1 Brief Analysis of Weighted Average Model by de Vries

First, Maxwell [22] published details of the ECM for a two-phase dispersion system consisting of randomly distributed and non-interacting uniform spheres immersed in a homogeneous continuous medium. Then, Fricke [23] and Burger [24] extended the application of this model to elongated spheroids. Eight years later, this model was customized by Eucken [25] to conduction heat transfer through multi-component systems. Subsequently, in 1952, Eucken's model [25] was further modified by de Vries [26] for estimating thermal conductivity of unsaturated soils. This specifically customized model was based on weighted average contributions of the basic components of the soil (quartz, other minerals, water, and air) which gave the first visible impression of a physical-based model. However, de Vries' 1952 model [26] was very complex due to the need to deal with two different continuous media (air and water); and therefore, it introduced numerous coefficients that were difficult to determine. In addition, the use of a soil weighting factor ( $\kappa_i$ ) introduced several implicit characteristics of soil structure that were not fulfilled in the soils. For example, it was assumed that all soil grains were of the same size and ellipsoidal in shape. It was also assumed that the soil grains are far apart from each other so that they have no contact with each other. These restrictions do not reflect real conditions in the field soils. However, apart from these limitations, it has been shown by de Vries [6] and Tarnawski [20] that  $\kappa_i$  can still be successfully applied to field soils after some modifications. This is probably the reason why, despite its complexity de Vries model, it is still frequently cited in the soil science literature as the top mechanistic model. However, the complexity of this model can be reduced considerably if a continuous phase of compacted soil minerals is considered. Indeed, the soil matrix is a key factor affecting the soil thermal conductivity [15, 21]. It is defined as a random collection of compacted solid particles, each with a unique shape and myriad irregular surfaces. A dominant heat pathway is via the soil grains, while the other potential heat pathways, via air and/or water account for a much smaller proportion of the total amount of heat transferred. Considering the above, the main objective of this paper is to develop a new weighted average model in which soil solids represent the continuous phase.

### 2.2 Weighted Average Models with Soil Solids as the Continuous Phase

Two weighted average models (deV-1 and deV-2), recently examined by Tarnawski [20], significantly underestimated soil thermal conductivity. As a result, they were customized by introducing complex expressions describing the latent heat effects due to migration of water vapor in soil air. For simplicity, this issue was disregarded in the development of new models with soil solids as the continuous medium.

### 2.2.1 Model with Continuous Phase made of Two Distinctive Mineral Groups: WAM<sub>s</sub>-1

Like the de Vries’ model [26], WAM<sub>s</sub>-1 includes weighted average contributions of the volumetric fractions ( $\theta_i$ ), thermal conductivities ( $\lambda_i$ ), and weighting factors ( $\kappa_i$ ) of the soil basic components, i.e., quartz, other minerals, water, and air. Then, the effective soil thermal conductivity ( $\lambda$ ) is estimated from Eq. 1.

$$\lambda = \frac{\kappa_w \cdot \theta_w \cdot \lambda_w + \kappa_a \cdot \theta_a \cdot \lambda_a + \kappa_{qtz} \cdot \theta_{qtz} \cdot \lambda_{qtz} + \kappa_{o-min} \cdot \theta_{o-min} \cdot \lambda_{o-min}}{\kappa_w \cdot \theta_w + \kappa_a \cdot \theta_a + \kappa_{qtz} \cdot \theta_{qtz} + \kappa_{o-min} \cdot \theta_{o-min}} \tag{1}$$

where  $\kappa_i$  is

$$\kappa_i = \frac{1}{3} \left[ \frac{2}{1 + \left(\frac{\lambda_i}{\lambda_s} - 1\right)g_i} + \frac{1}{1 + \left(\frac{\lambda_i}{\lambda_s} - 1\right)(1 - 2g_i)} \right] \tag{2}$$

where  $g$  is control factor and the subscript  $s$  represents continuous medium, i.e., soil solids.

The main innovation of this model is based on the hypothesis that the continuous phase consists of soil minerals, divided into two distinctive groups; namely, quartz and other minerals while soil water and air were considered as the dispersed phase.

The heat flux through the continuous phase was characterized by its thermal conductivity, i.e., soil solids ( $\lambda_s$ ), which can be evaluated by a geometric mean model [15].

$$\lambda_s = \lambda_{qtz}^{\Theta_{qtz}} \cdot (\lambda_{o-min})^{1-\Theta_{qtz}} \tag{3}$$

where  $\Theta_{qtz}$  is the volumetric fraction of quartz in the soil solids.

Then, thermal conductivity of other minerals ( $\lambda_{o-min}$ ) was obtained from [15], i.e., the geometric mean relation applied to the thermal conductivity of fully saturated soils ( $\lambda_{sat}$ ).

$$\lambda_{o-min} = \left[ (\lambda_{sat} / \lambda_w^n)^{\frac{1}{1-n}} / \lambda_{qtz}^{\Theta_{qtz}} \right]^{1/(1-\Theta_{qtz})} \tag{4}$$

The weighting factor  $\kappa$ , for basic soil components made of ellipsoidal particles, has the following forms:

$$\kappa_{qtz} = \frac{1}{3} \left[ \frac{2}{1 + \left(\frac{\lambda_{qtz}}{\lambda_s} - 1\right)g_{qtz}} + \frac{1}{1 + \left(\frac{\lambda_{qtz}}{\lambda_s} - 1\right)(1 - 2g_{qtz})} \right] \tag{5}$$

$$\kappa_{o-\min} = \frac{1}{3} \left[ \frac{2}{1 + \left(\frac{\lambda_{o-\min}}{\lambda_s} - 1\right)g_{o-\min}} + \frac{1}{1 + \left(\frac{\lambda_{o-\min}}{\lambda_s} - 1\right)(1 - 2g_{o-\min})} \right] \tag{6}$$

$$\kappa_w = \frac{1}{3} \left[ \frac{2}{1 + \left(\frac{\lambda_w}{\lambda_s} - 1\right)g_w} + \frac{1}{1 + \left(\frac{\lambda_w}{\lambda_s} - 1\right)(1 - 2g_w)} \right] \tag{7}$$

$$\kappa_a = \frac{1}{3} \left[ \frac{2}{1 + \left(\frac{\lambda_a}{\lambda_s} - 1\right)g_a} + \frac{1}{1 + \left(\frac{\lambda_a}{\lambda_s} - 1\right)(1 - 2g_a)} \right] \tag{8}$$

where the control factor for other minerals is assessed as follows [20]:

$$g_{o-\min} = m_{sa} \cdot g_{sa} + m_{si} \cdot g_{si} + m_{cl} \cdot g_{cl} \tag{9}$$

The WAM<sub>s</sub>-1 offers a noticeable simplicity with respect to deV-1, i.e., a lack of complex and controversial expressions for migration of water vapor in soil air carrying latent heat, an absence of a controversial switching point  $\theta_{cr}$  between air and water as a continuous phase, and a complete elimination of discontinuity in  $\lambda$  as a function of  $S_r$ ,  $\lambda(S_r)$ , at the switching point. Consequently, the WAM<sub>s</sub>-1 structure is simple and the model is straightforward to follow and apply.

### 2.2.2 Model with Continuous Phase Considering all Soil Minerals: WAM<sub>s</sub>-2

The effective soil thermal conductivity can also be estimated by considering all soil solids (minerals) as the continuous phase. Hence, the weighting factor for the soil solids becomes unity ( $\kappa_s = 1$ ). Therefore, Eq. 1 is further simplified to the following form:

$$\lambda = \frac{\kappa_w \cdot \theta_w \cdot \lambda_w + \kappa_a \cdot \theta_a \cdot \lambda_a + \theta_s \cdot \lambda_s}{\kappa_w \cdot \theta_w + \kappa_a \cdot \theta_a + \theta_s} \tag{10}$$

After substituting Eq. 3 into Eq. 10, the following expression was obtained:

$$\lambda = \frac{\kappa_w \cdot \theta_w \cdot \lambda_w + \kappa_a \cdot \theta_a \cdot \lambda_a + \theta_s \cdot \lambda_{qtz}^{\Theta_{qtz}} \cdot (\lambda_{o-\min})^{1-\Theta_{qtz}}}{\kappa_w \cdot \theta_w + \kappa_a \cdot \theta_a + \theta_s} \tag{11}$$

Only two weighting factors are required,  $\kappa_w$  and  $\kappa_a$ , as defined by Eqs. 7 and 8. With this regard, the WAM<sub>s</sub>-2 is noticeably simpler than WAM<sub>s</sub>-1 as it does not require soil control factors for quartz ( $g_{qtz}$ ) and other minerals ( $g_{o-\min}$ ). The only control parameters required are  $g_w$  and  $g_a$ , for evaluating the weighting factors  $\kappa_w$  and  $\kappa_a$ .

## 2.3 Soil Thermal Conductivity Database

A comprehensive soil database is needed to assess two new models for soil thermal conductivity. This type of database should include the following information: fractions of grain size distribution for clay, silt, and sand (i.e.,  $m_{cl}$ ,  $m_{si}$ ,  $m_{sa}$ ), soil porosity ( $n$ ), mineral composition ( $\theta_{min}$ ), density of soil solids ( $\rho_s$ ), volumetric water content ( $\theta_w$ ) or degree of saturation ( $S_r$ ), and experimentally measured thermal conductivity data. Currently, the above requirements are solely met by the Canadian soil database [17, 20, 27]. The other databases on thermal conductivity of soils usually do not contain complete information on mineral composition and thermal conductivity data at dryness and saturation are often not available. The next subsection provides a summary of the 40 Canadian Soils thermal conductivity database, i.e., 39 field soils and one pure quartz sand from Sable Island (Atlantic Canada). For details of the 40 Canadian Soils database and the experimental methods see Tarnawski [17, 27].

### 2.3.1 Canadian Soils Database

Forty field soil samples, from nine Canadian provinces, were subjected to non-stationary thermal conductivity tests under laboratory conditions. The texture of seven soil samples from Nova Scotia (NS) varied from coarse to silty. Three soil samples from Prince Edward Island (PE) were mainly loamy sand. Five soil samples from New Brunswick (NB) were mainly silty loam or silty clay loam. Two soil samples from Quebec (QC) were coarse-grained (sand and loamy sand). The texture of seven soil samples from Ontario (ON) ranged from sand to silt loam. Four soil samples from Manitoba (MN) were loamy sand to silt loam. Five soil samples from Saskatchewan (SK) were loamy sand or silt loam. One soil sample from Alberta (AB) was silty loam. All six samples from British Columbia (BC) were generally fine soils, ranging from silty loam to silty clay loam. Each soil sample was tested nine times, with an overall uncertainty of  $\pm 6.3\%$  at 95% confidence level, at each  $S_r$  value (i.e.,  $S_r=0, 0.1, 0.25, 0.5, 0.7$  and 1), under laboratory conditions, to obtain the one average thermal conductivity value. The basic data on the grain size distribution of the soil and the complete thermal conductivity data were summarized in Tarnawski [17, 27]. A summary of the mineral occurrence in the 39 Canadian Field Soils and a corresponding summary for  $\lambda_{o-min}$  and  $\lambda_s$  can be found in Tarnawski [17, 27].

### 2.3.2 Standard Sands Database

The complete physical data of the standard sands (C-109, C-190, and NS-04) were given by Tarnawski [28, 29]. C-109 and C-190 are natural silica sands (99.8% quartz) with rounded or sub-rounded shape grains, while NS-04 is pure quartz sand from Sable Island (Atlantic Canada). A summary of the complete thermal conductivity data of three Standard Sands can be found in [28, 29].



### 2.4 Model Calibration Procedure

The model estimates ( $\lambda_{est}$ ) were compared with experimental data ( $\lambda_{exp}$ ) and the standard deviation ( $SD$ ) was used as a measure of the model performance, defined as follows:

$$SD = \sqrt{\frac{1}{N - M} \sum_1^N (\lambda_{exp} - \lambda_{est})^2} \tag{12}$$

where  $M$  is the number of presently fitted coefficients in the WAMs and  $N$  is the total number of sampled data.

#### 2.4.1 WAM<sub>5</sub>-1

The model control parameters ( $g_{qtz}$ ,  $g_{sa}$ ,  $g_{si}$ ,  $g_{cl}$ , and  $g_w$ ) were assumed to be the same as for deV-1, i.e., they were already previously determined by fitting to  $\lambda$  data from 39 Canadian Field Soils [20]. So, consequently, they do not presently contribute to  $M$  because they are already known.

Table 1 summarizes the previously fitted factors for soil grains ( $g_i$ ) and water ( $g_w$ ). The fitted factor  $g_{qtz} = 0.15$  was used only to evaluate  $\kappa_{qtz}$ , while the other  $g_i$  values, corresponding to soil texture: sandy ( $0.5 < m_{sa} \leq 1$ ), silty ( $0.5 \leq m_{sa} \leq 0.1$ ), and clayey ( $m_{sa} < 0.1$ ), were used to evaluate  $\kappa_{o-min}$ .

The remaining model control factor is the soil air coefficient ( $g_a$ ) which is particularly important due to the elimination of the latent heat effects of water vapor in soil air. Therefore, it is useful to reveal details on the procedure for fitting and calculating  $g_a$ . First, it was assumed that the  $g_a$  values were the same as in deV-1. Next,  $\lambda_{est}$  was calculated for all  $S_r$  values ( $S_r = 0, 0.1, 0.25, 0.5, 0.7, \text{ and } 1$ ) and the corresponding average  $SD$ s were obtained. Then,  $g_a$  values were adjusted at each  $S_r$  value, keeping the smallest total  $SD$ . Next, a dynamic plot of  $g_a$  versus  $S_r$  was made for 17 coarse and 22 fine soils and the final  $g_a$  adjustment, combined with a  $g_a(S_r)$  curve fit, was performed. Finally, the following  $g_a$  equations were obtained for 17 coarse and 22 fine soils, minimizing the  $SD$  between  $\lambda_{est}$  and  $\lambda_{exp}$ .

Coarse soils ( $m_{sa} > 0.5$ ):

$$g_a = 0.0035 - 0.0267 \cdot S_r + 1.1186 \cdot S_r^2 - 3.3481 \cdot S_r^3 + 3.8429 \cdot S_r^4 - 1.5169 \cdot S_r^5 \quad R^2 = 1.0 \tag{13}$$

**Table 1** Fitted control factors: grains ( $g_i$ ) [20]

Texture	Quartz	Sand	Silt	Clay	Water
$g_i$	0.150	0.120	0.090	0.0750	0.0001

Fine soils ( $m_{sa} \leq 0.5$ ):

$$g_a = 0.005 - 0.0194 \cdot S_r + 0.7168 \cdot S_r^2 - 1.9042 \cdot S_r^3 + 2.0573 \cdot S_r^4 - 0.7986 \cdot S_r^5 \quad R^2 = 1.0 \quad (14)$$

#### 2.4.2 Standard Sands (NS-04, C-109, and C-190)

The grains of pure quartz sands (NS-04, C-109, and C-190) are larger and more uniform in size, compared to ordinary field soils; therefore, they require different  $g_a$  and  $g_w$  values. Below is a function of  $g_a$  versus  $S_r$  obtained by fitting to the thermal conductivity data of the Standard Sands, while minimizing  $SD$ .

Pure quartz sands:

$$g_a = 0.05674 \cdot S_r^{0.3053} \quad R^2 = 0.9904 \quad (15)$$

For  $g_w = 0.0001$  and  $g_a$  as above, underestimates of thermal conductivity were observed at  $S_r > 0.5$ . To minimize this problem, a new function  $g_w(S_r)$  was introduced:

Pure quartz sands:

$$g_w = 0.001 + 0.02252 \cdot S_r \quad R^2 = 0.995 \quad (16)$$

#### 2.4.3 WAM<sub>s</sub>-2

The WAM<sub>s</sub>-2 assumes that all soil minerals are consolidated and form the continuous phase. For this reason, the model structure (Eq. 1) is further simplified by  $\kappa_s = 1$  (according to Eq. 2). Consequently, the control parameters for the soil solids ( $g_{qtz}$ ,  $g_{sa}$ ,  $g_{si}$ , and  $g_{cl}$ ) were eliminated. Then, the control parameter for soil water ( $g_w$ ) was assumed to be the same as for deV-1 and for WAM<sub>s</sub>-1, leaving  $g_a$  as the only control parameter which was assumed to be the same as for WAM<sub>s</sub>-1, since both the models are based on the same continuous phase of soil solids (i.e., soil minerals).

### 3 Results

The following guiding principles for the model performance ( $SD$  values) were recently established [17]:

- Superior performance:  $SD < 0.1 \text{ W} \cdot \text{m}^{-1} \cdot \text{K}^{-1}$
- Good performance:  $0.1 \leq SD \leq 0.15 \text{ W} \cdot \text{m}^{-1} \cdot \text{K}^{-1}$
- Satisfactory performance:  $0.15 < SD \leq 0.25 \text{ W} \cdot \text{m}^{-1} \cdot \text{K}^{-1}$

- Poor performance:  $SD > 0.25 \text{ W}\cdot\text{m}^{-1}\cdot\text{K}^{-1}$

### 3.1 Canadian Field Soils

Table 2 summarizes the model predictive performance of  $\text{WAM}_s\text{-1}$ ,  $\text{WAM}_s\text{-2}$ , and  $\text{deV-1}$  for 17 coarse soils, 22 fine soils, and all 39 Canadian Field Soils. The  $SD$  data for  $\text{WAM}_s\text{-1}$  ( $M=6$ , due to six fitted polynomial coefficients of Eq. 13 or 14) were compared with  $SD$  records for  $\text{WAM}_s\text{-2}$  ( $M=6$ , due to six fitted polynomial coefficients of Eq. 13 or 14) and  $\text{deV-1}$  ( $M=7$ ).

For 17 coarse soils, 22 fine soils, and all 39 soils, the  $\lambda_{\text{est}}$  by the two new models (with  $\lambda_{\text{qtz}}=7.6 \text{ W}\cdot\text{m}^{-1}\cdot\text{K}^{-1}$  and  $\lambda_a=0.026 \text{ W}\cdot\text{m}^{-1}\cdot\text{K}^{-1}$ ) are approximately in the  $SD$  range which corresponds to good/superior model performance. This result confirms that the superior values of  $SD$  can be achieved even without considering the latent heat effects due to water vapor migration in soils. For  $\text{WAM}_s\text{-1}$  and  $\text{WAM}_s\text{-2}$ , the average  $SD$ s are  $\pm 0.110$  and  $\pm 0.135 \text{ W}\cdot\text{m}^{-1}\cdot\text{K}^{-1}$  for 17 coarse soils,  $\pm 0.054$  and  $\pm 0.069 \text{ W}\cdot\text{m}^{-1}\cdot\text{K}^{-1}$  for 22 fine soils, and  $\pm 0.078$  and  $\pm 0.098 \text{ W}\cdot\text{m}^{-1}\cdot\text{K}^{-1}$  for all 39 soils. For  $\text{deV-1}$  (with  $\lambda_{\text{qtz}}=7.6 \text{ W}\cdot\text{m}^{-1}\cdot\text{K}^{-1}$  and  $\lambda_{a\text{-app}}=\lambda_a+\lambda_v$ , where  $\lambda_{a\text{-app}}$  is the apparent thermal conductivity of humid soil air [20]), average  $SD$ s of  $\pm 0.103 \text{ W}\cdot\text{m}^{-1}\cdot\text{K}^{-1}$  were obtained for 17 coarse soils,  $\pm 0.087 \text{ W}\cdot\text{m}^{-1}\cdot\text{K}^{-1}$  for 22 fine soils, and  $\pm 0.094 \text{ W}\cdot\text{m}^{-1}\cdot\text{K}^{-1}$  for all 39 soils; these  $SD$ s correspond to superior/good levels.

Figures 1, 2, 3, and 4 show some examples of the worst  $\lambda_{\text{est}}(S_r)$  produced by  $\text{deV-1}$ ,  $\text{WAM}_s\text{-1}$ , and  $\text{WAM}_s\text{-2}$ . The Nova Scotia soil (NS-05), Fig. 1, belongs to the group of coarse texture with a high content of quartz ( $\theta_{\text{qtz}}=0.72$ ); consequently, a high value of  $\lambda_{\text{exp}} \approx 2.4 \text{ W}\cdot\text{m}^{-1}\cdot\text{K}^{-1}$  is observed at  $S_r=1$ . The following  $SD$ s were obtained:  $\text{deV-1}$ :  $\pm 0.073 \text{ W}\cdot\text{m}^{-1}\cdot\text{K}^{-1}$ ,  $\text{WAM}_s\text{-1}$ :  $\pm 0.182 \text{ W}\cdot\text{m}^{-1}\cdot\text{K}^{-1}$ , and  $\text{WAM}_s\text{-2}$ :  $\pm 0.177 \text{ W}\cdot\text{m}^{-1}\cdot\text{K}^{-1}$ . In general, the obtained  $\lambda_{\text{est}}$  closely followed the trend of  $\lambda_{\text{exp}}(S_r)$  with an overestimation in the low  $S_r$  range ( $S_r \approx 0.1$ ) and an underestimation at  $S_r \approx 1$ .

The Ontario soil (ON-04), Fig. 2, is a coarse sand ( $m_{\text{sa}}=0.89$ ) with a relatively low quartz content ( $\theta_{\text{qtz}}=0.38$ ). All three models provide good/acceptable estimates. The  $\lambda_{\text{est}}$  of all models agree well with the experimental data at  $S_r=0$  and  $S_r > 0.7$ . Underestimates of the thermal conductivity were observed in the remaining  $S_r$  range.

Figure 3 shows the modeling results for MN-02 (silty loam:  $m_{\text{sa}}=0.217$ ). Despite a low content of quartz ( $\theta_{\text{qtz}}=0.20$ ), its  $\lambda_{\text{sat}}$  was about  $2.2 \text{ W}\cdot\text{m}^{-1}\cdot\text{K}^{-1}$ . The high values of thermal conductivity are due to a high content of calcite and dolomite ( $\theta_{\text{cal}}=0.28$ ,  $\theta_{\text{dol}}=0.37$ ); both minerals have thermal conductivity

**Table 2** Canadian soils: model performance ( $SD$  in  $\text{W}\cdot\text{m}^{-1}\cdot\text{K}^{-1}$ )

Model	$SD_{17\text{-coarse}}$	$SD_{22\text{-fine soils}}$	$SD_{39\text{soils}}$
$\text{WAM}_s - 1$	0.110	0.054	0.078
$\text{WAM}_s - 2$	0.135	0.069	0.098
$\text{deV-1}$	0.103	0.087	0.094

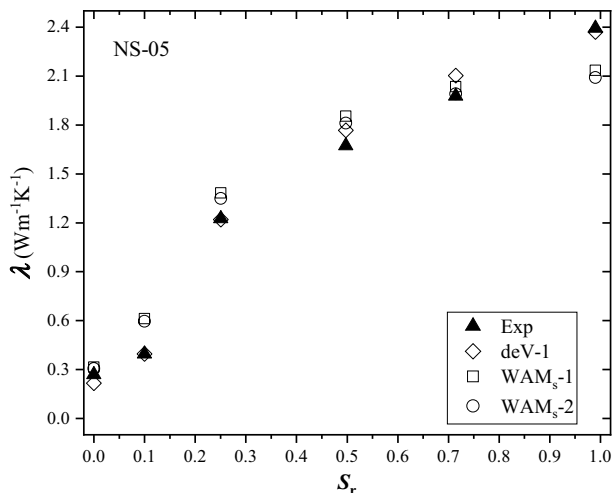


**Fig. 1** Nova Scotia soil (NS-05):  $\lambda$  vs.  $S_r$ ,  $m_{sa}=0.85$ ,  $\theta_{qtz}=0.72$ ,  $n=0.40$ , ( $SD_{deV-1}=0.073 \text{ W}\cdot\text{m}^{-1}\cdot\text{K}^{-1}$ ,  $SD_{WAMs-1}=0.182 \text{ W}\cdot\text{m}^{-1}\cdot\text{K}^{-1}$ ,  $SD_{WAMs-2}=0.177 \text{ W}\cdot\text{m}^{-1}\cdot\text{K}^{-1}$ )

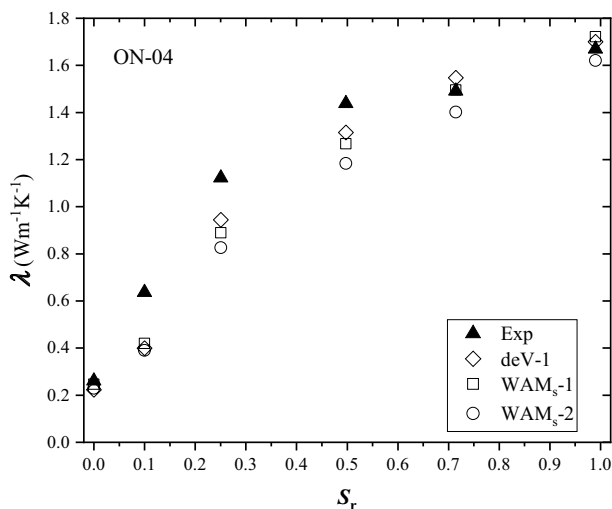


**Fig. 2** Ontario soil (ON-04):  $\lambda$  vs.  $S_r$ ,  $m_{sa}=0.89$ ,  $\theta_{qtz}=0.38$ ,  $n=0.39$ , ( $SD_{deV-1}=0.144 \text{ W}\cdot\text{m}^{-1}\cdot\text{K}^{-1}$ ,  $SD_{WAMs-1}=0.157 \text{ W}\cdot\text{m}^{-1}\cdot\text{K}^{-1}$ ,  $SD_{WAMs-2}=0.205 \text{ W}\cdot\text{m}^{-1}\cdot\text{K}^{-1}$ )

values of  $3.03 \text{ W}\cdot\text{m}^{-1}\cdot\text{K}^{-1}$  and  $5.07 \text{ W}\cdot\text{m}^{-1}\cdot\text{K}^{-1}$ , respectively. The two  $WAM_s$  models had slightly underestimated thermal conductivity values throughout the  $S_r$  range, except at  $S_r=0$  and  $0.7$ , which were slightly overestimated;  $SD$  values were  $\pm 0.105 \text{ W}\cdot\text{m}^{-1}\cdot\text{K}^{-1}$  for  $WAM_s-1$  and  $\pm 0.110 \text{ W}\cdot\text{m}^{-1}\cdot\text{K}^{-1}$  for  $WAM_s-2$ . The

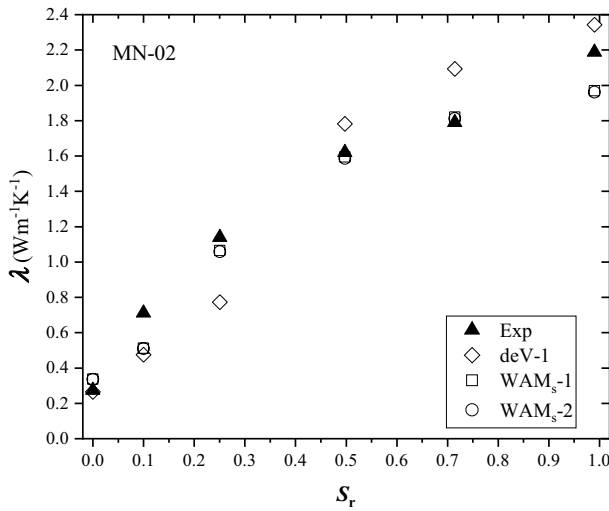


**Fig. 3** Manitoba soil (MN-02):  $\lambda$  vs.  $S_r$ ,  $m_{sa}=0.217$ ,  $\theta_{qtz}=0.20$ ,  $\theta_{cal}=0.28$ ,  $\theta_{dol}=0.37$ ,  $n=0.41$ , ( $SD_{deV-1}=0.252 \text{ W}\cdot\text{m}^{-1}\cdot\text{K}^{-1}$ ,  $SD_{WAMs-1}=0.105 \text{ W}\cdot\text{m}^{-1}\cdot\text{K}^{-1}$ ,  $SD_{WAMs-2}=0.110 \text{ W}\cdot\text{m}^{-1}\cdot\text{K}^{-1}$ )

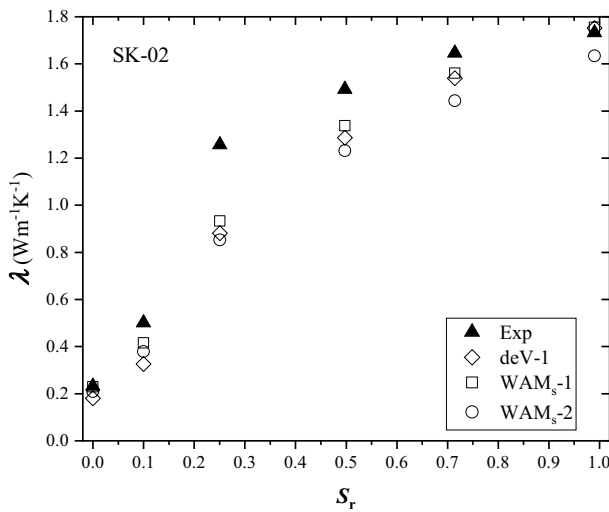


**Fig. 4** Saskatchewan soil (SK-02):  $\lambda$  vs.  $S_r$ ,  $m_{sa}=0.67$ ,  $\theta_{qtz}=0.61$ ,  $n=0.45$ , ( $SD_{deV-1}=0.209 \text{ W}\cdot\text{m}^{-1}\cdot\text{K}^{-1}$ ,  $SD_{WAMs-1}=0.164 \text{ W}\cdot\text{m}^{-1}\cdot\text{K}^{-1}$ ,  $SD_{WAMs-2}=0.236 \text{ W}\cdot\text{m}^{-1}\cdot\text{K}^{-1}$ )

$SD$  value of  $\pm 0.252 \text{ W}\cdot\text{m}^{-1}\cdot\text{K}^{-1}$  was obtained for deV-1, which falls within the poor performance range.

Figure 4 shows the  $\lambda_{est}$  for SK-02 (silt loam) which achieved the worst result among the 39 Canadian soils. All three models performed poorly at  $S_r=0.25$  and  $S_r=0.50$ , while good  $\lambda_{est}$  were obtained for soil dryness and soil saturation.

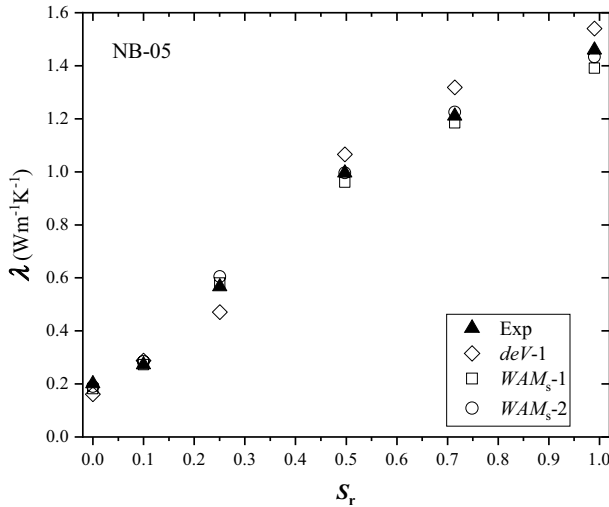


**Fig. 5** New Brunswick soil (NB-05):  $\lambda$  vs.  $S_r$ ,  $m_{cl}=0.33$ ,  $m_{si}=0.67$ ,  $\theta_{qtz}=0.39$ ,  $n=0.54$ , ( $SD_{deV-1}=0.080 \text{ W}\cdot\text{m}^{-1}\cdot\text{K}^{-1}$ ,  $SD_{WAMs-1}=0.022 \text{ W}\cdot\text{m}^{-1}\cdot\text{K}^{-1}$ ,  $SD_{WAMs-2}=0.037 \text{ W}\cdot\text{m}^{-1}\cdot\text{K}^{-1}$ )

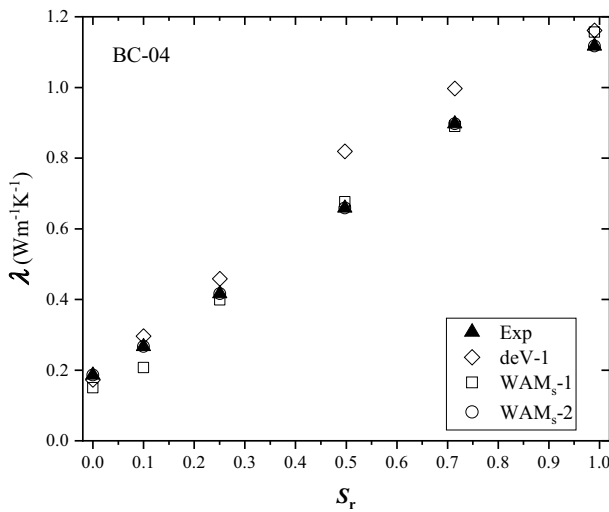
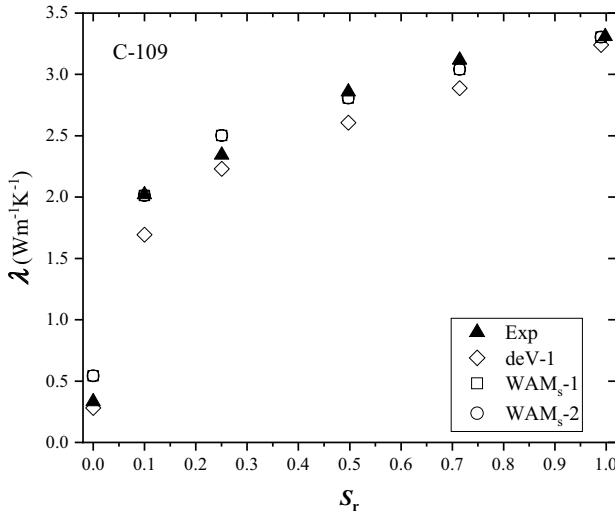


**Fig. 6** British Columbia soil (BC-04):  $\lambda$  vs.  $S_r$ ,  $m_{cl}=0.41$ ,  $m_{si}=0.59$ ,  $\theta_{qtz}=0.17$ ,  $n=0.52$ , ( $SD_{deV-1}=0.088 \text{ W}\cdot\text{m}^{-1}\cdot\text{K}^{-1}$ ,  $SD_{WAMs-1}=0.035 \text{ W}\cdot\text{m}^{-1}\cdot\text{K}^{-1}$ ,  $SD_{WAMs-2}=0.043 \text{ W}\cdot\text{m}^{-1}\cdot\text{K}^{-1}$ )

Figures 5 and 6 show two examples of the superior performance of the models. The New Brunswick soil (NB-05) is a fine-textured soil ( $m_{sa}=0$ ) for which the thermal conductivity is best estimated by all three models (Fig. 5), although the thermal conductivity is slightly underestimated at soil dryness. In particular, the  $\lambda_{est}$  of WAM<sub>s</sub>-1 and WAM<sub>s</sub>-2 followed the experimental data very closely over the whole  $S_r$  range, while the estimates of deV-1 showed increasing overestimates for  $S_r > 0.5$ .

**Table 3** Standard sands: model performance ( $SD$  in  $W \cdot m^{-1} \cdot K^{-1}$ )

Code	C-109 ( $n=0.32$ )	C-109 ( $n=0.36$ )	C-109 ( $n=0.40$ )	NS-04 ( $n=0.36$ )	C-190 ( $n=0.32$ )	C-190 ( $n=0.36$ )	C-190 ( $n=0.40$ )	$SD_{ave}$
deV-1	0.246	0.168	0.249	0.283	0.207	0.168	0.194	0.216
WAM <sub>s</sub> -1	0.098	0.163	0.117	0.139	0.118	0.158	0.121	0.131
WAM <sub>s</sub> -2	0.098	0.163	0.117	0.139	0.118	0.158	0.121	0.131



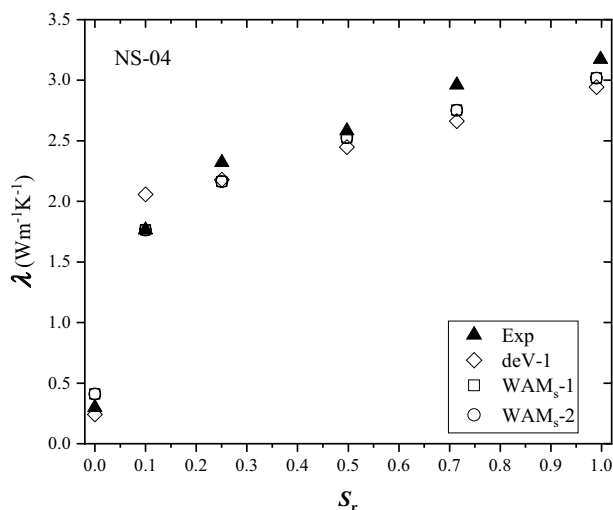
**Fig. 7** Ottawa sand (C-109):  $\lambda$  vs.  $S_r$ ,  $m_{sa}=1.00$ ,  $\theta_{qtz}=1.00$ ,  $n=0.32$ , ( $SD_{deV-1}=0.109 W \cdot m^{-1} \cdot K^{-1}$ ,  $SD_{WAMs-1}=0.098 W \cdot m^{-1} \cdot K^{-1}$ ,  $SD_{WAMs-2}=0.096 W \cdot m^{-1} \cdot K^{-1}$ )

Figure 6 shows the close agreement of  $\lambda_{est}$  and  $\lambda_{exp}$  of all models for clayey soil (BC-04), which also has a fine texture. Again, the predictive performance ( $SD$ ) of all three models falls into the superior category, i.e.,  $SD < 0.1 W \cdot m^{-1} \cdot K^{-1}$ . In particular,  $\lambda_{est}$  of WAM<sub>s</sub>-1 and WAM<sub>s</sub>-2 followed the trend of experimental data very closely throughout the  $S_r$  range with slight underestimates of thermal conductivity observed at soil dryness.

### 3.2 Standard Sands

Table 3 summarizes average  $SD$  for deV-1 ( $\theta_{cr}=0.0625 n$ ;  $\lambda_{a-app}=\lambda_a+\lambda_v$ ), WAM<sub>s</sub>-1 and WAM<sub>s</sub>-2; the  $SD$  comparison was made using  $\lambda_{qtz}=7.6 W \cdot m^{-1} \cdot K^{-1}$ . It is obvious that the closest  $\lambda_{est}$  were given by WAM<sub>s</sub>-1 and WAM<sub>s</sub>-2, while  $\lambda_{est}$  by deV-1 were noticeably worse in comparison. At soil dryness, obtained estimates of  $\lambda$  consistently showed inflated values above  $\lambda_{dry-exp}$ .

Figure 7 shows the modeling results compared to the experimental data for C-109. The obtained average  $SDs$  were  $\pm 0.109 W \cdot m^{-1} \cdot K^{-1}$  for deV-1,  $\pm 0.098 W \cdot m^{-1} \cdot K^{-1}$



**Fig. 8** Sable Island sand (NS-04):  $\lambda$  vs.  $S_r$ ,  $m_{sa}=1.0$ ,  $\theta_{qtz}=1.0$ ,  $n=0.36$ , ( $SD_{deV-1}=0.180 \text{ W}\cdot\text{m}^{-1}\cdot\text{K}^{-1}$ ,  $SD_{WAM_s-1}=0.139 \text{ W}\cdot\text{m}^{-1}\cdot\text{K}^{-1}$ ,  $SD_{WAM_s-2}=0.135 \text{ W}\cdot\text{m}^{-1}\cdot\text{K}^{-1}$ )

for  $WAM_s-1$  and  $\pm 0.096 \text{ W}\cdot\text{m}^{-1}\cdot\text{K}^{-1}$  for  $WAM_s-2$ , which are good/superior  $\lambda$  estimates.

Figure 8 shows the modeling results compared to the experimental data for NS-04 (100% pure quartz). Again, the  $WAM_s-1$  and  $WAM_s-2$  models offered similar  $SD$  data and their thermal conductivity trends closely followed the experimental data. In general, the average  $SD$ s were  $\pm 0.180 \text{ W}\cdot\text{m}^{-1}\cdot\text{K}^{-1}$  for deV-1,  $\pm 0.139 \text{ W}\cdot\text{m}^{-1}\cdot\text{K}^{-1}$  for  $WAM_s-1$  and  $\pm 0.135 \text{ W}\cdot\text{m}^{-1}\cdot\text{K}^{-1}$  for  $WAM_s-2$ , which is a good predictive performance.

### 3.3 Application to 10 Chinese Soils

Both  $WAM_s$  with fixed parameters ( $g_{qtz}$ ,  $g_{sa}$ ,  $g_{si}$ ,  $g_{cl}$ ,  $g_w$ , and  $g_a$ ) were applied to the thermal conductivity data of 10 Chinese soils [13], divided into two groups: coarse ( $m_{sa} > 0.5$ ) and fine ( $m_{sa} \leq 0.5$ ). The quartz content,  $\theta_{qtz}$ , was estimated by applying an iterative fit of  $\lambda_{est}$  to experimental  $\lambda$  data [30]. The basic physical characteristics of soil were summarized by Tarnawski [20]. The  $\lambda_{est}$  were determined by assuming the following data:  $\lambda_{qtz} = 7.6 \text{ W}\cdot\text{m}^{-1}\cdot\text{K}^{-1}$  and  $\lambda_{o-min} = 2.12 \text{ W}\cdot\text{m}^{-1}\cdot\text{K}^{-1}$ . For deV-1, the following constraints were applied:  $M=7$  and  $\theta_{cr}$  values according to  $m_{sa}$ : 0.023 ( $m_{sa} = 1.0$ ); 0.05 ( $0.50 < m_{sa} < 1.0$ ); 0.10 ( $0.15 < m_{sa} < 0.5$ ); and 0.15 ( $m_{sa} < 0.15$ ). A summary of average  $SD$  values for deV-1,  $WAM_s-1$ , and  $WAM_s-2$  can be found in Table 4.



**Table 4** Chinese soils: model performance (*SD* in  $W \cdot m^{-1} \cdot K^{-1}$ )

Soil code	deV-1	Ave	WAM <sub>s</sub> -1	Ave	WAM <sub>s</sub> -2	Ave
S-Ren-001	0.186		0.236		0.277	
S-Ren-002	0.090		0.156		0.193	
S-Ren-003	0.141		0.135		0.179	
S-Ren-011	0.044	0.115	0.217	0.186	0.164	0.203
S-Ren-004	0.156		0.192		0.229	
S-Ren-005	0.132		0.069		0.080	
S-Ren-006	0.162		0.263		0.296	
S-Ren-007	0.067		0.076		0.102	
S-Ren-008	0.143		0.091		0.120	
S-Ren-009	0.101	0.127	0.124	0.136	0.081	0.151
Ave	0.122		0.156		0.172	

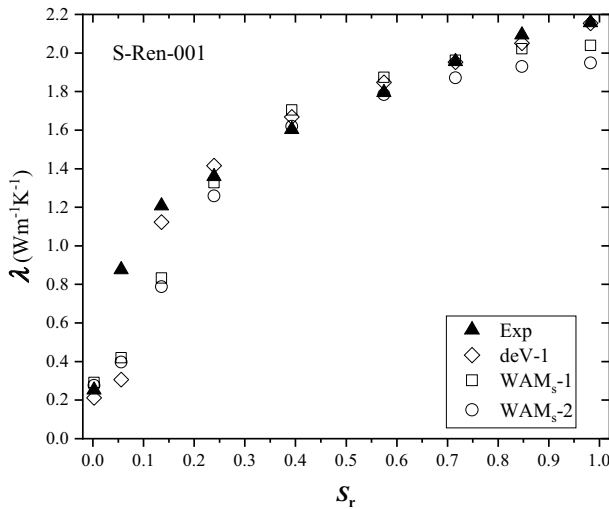


**Fig. 9** Chinese soil (S-Ren-001):  $\lambda$  vs.  $S_r$ ,  $m_{sa}=0.94$ ,  $\theta_{qiz}=0.74$ ,  $n=0.408$ , ( $SD_{deV-1}=0.186 W \cdot m^{-1} \cdot K^{-1}$ ,  $SD_{WAMs-1}=0.236 W \cdot m^{-1} \cdot K^{-1}$ ,  $SD_{WAMs-2}=0.277 W \cdot m^{-1} \cdot K^{-1}$ )

Typical trends of  $\lambda_{est}$  versus  $S_r$  are shown in Fig. 9 and 10. The WAM<sub>s</sub>-1 model underestimated the experimental data at  $0.06 < S_r < 0.20$  (Fig. 9), while  $\lambda_{est}$  of deV-1 closely follows the experimental data, with an exception at  $S_r = 0.06$ , where the largest underestimation is observed. For both WAM<sub>s</sub> models, the average *SDs* are within acceptable predictive performance. The WAM<sub>s</sub>-1 estimates closely follow the experimental data (Fig. 10). The average *SDs*, for both models, are within good predictive performance, while deV-1 underestimates  $\lambda_{exp}$  within  $0.15 < S_r < 0.3$ .

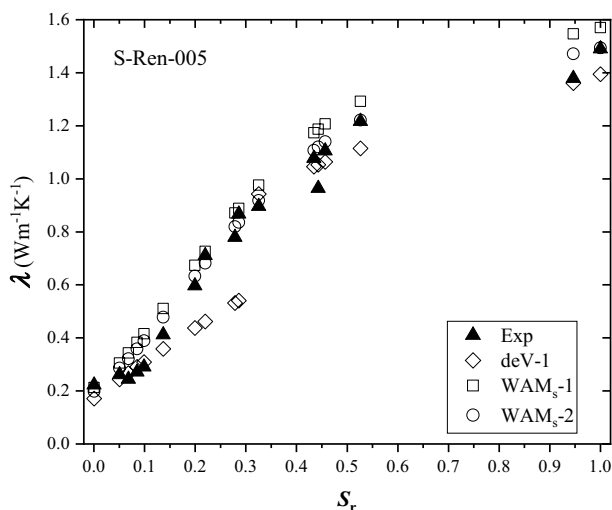


**Fig. 10** Chinese soil (S-Ren-005):  $\lambda$  vs.  $S_r$ ,  $m_{sa}=0.27$ ,  $\theta_{qtz}=0.55$ ,  $n=0.51$ , ( $SD_{deV-1}=0.132 \text{ W}\cdot\text{m}^{-1}\cdot\text{K}^{-1}$ ,  $SD_{WAM_s-1}=0.069 \text{ W}\cdot\text{m}^{-1}\cdot\text{K}^{-1}$ ,  $SD_{WAM_s-2}=0.080 \text{ W}\cdot\text{m}^{-1}\cdot\text{K}^{-1}$ )

## 4 Discussion

The two novel models were compared with deV-1 in terms of simplicity, quality of thermal conductivity estimates, and extension to other soils of different genesis and location. Concerning the model simplicity: the  $WAM_s-2$ , where all soil minerals are consolidated and form the continuous phase, offers the simplest structure and is therefore, very straightforward to use, i.e., only one soil air factor ( $g_a$ ) required fitting to experimental thermal conductivity data. The  $WAM_s-1$  offered a very similar structure to the  $WAM_s-2$ , but it considered soil solids divided into two different groups: quartz and other minerals and is therefore slightly more complex in structure than  $WAM_s-2$ . Furthermore, it does not require any adjustments for  $g_{qtz}$ ,  $g_{sa}$ ,  $g_{si}$ ,  $g_{cl}$ , and  $g_w$ , as they were assumed to be the same as in the deV-1 model. Therefore, both  $WAM_s-1$  and  $WAM_s-2$  were more straightforward than the original de Vries model (deV-1), which is more complex, more difficult to apply and more prone to manipulation. In deV-1, the final adjustment of the critical moisture content ( $\theta_{cr}$ ), corresponding to the switching point of the continuous medium (i.e., from air to water), is done a posteriori, when preliminary  $\lambda_{est}$  have been obtained; i.e., a value of  $\theta_{cr}$  is shifted up or down to obtain a minimum  $SD$  average. However, for soils without complete  $\lambda_{exp}$  data, guessed values of  $\theta_{cr}$  would have to be used. In this case, the deV-1 model might not perform well because of the uncertainty in  $\theta_{cr}$ . In contrary to deV-1, this problem does not exist for  $WAM_s-1$  and  $WAM_s-2$ . Furthermore, the deV-1 model required the use of apparent thermal conductivity of humid soil air, i.e., enhanced  $\lambda_a$  that includes the latent heat effects of water vapor. In contrast to deV-1 model, both  $WAM_s$  models use only  $\lambda_a$ , i.e., without latent heat effects due to the migration of soil water vapor. Regarding the model estimates quality,  $WAM_s-1$  provided more

accurate  $\lambda_{\text{est}}$  than WAM<sub>s</sub>-2 and deV-1, mainly due to a more appropriate representation of the soil solid phase which consist of quartz and other soil minerals. When both WAM<sub>s</sub> models were applied to 39 Canadian Soils, their average standard deviations (*SDs*) were as follows:  $\pm 0.110/0.135 \text{ W}\cdot\text{m}^{-1}\cdot\text{K}^{-1}$  for 17 coarse soils,  $\pm 0.054/0.069 \text{ W}\cdot\text{m}^{-1}\cdot\text{K}^{-1}$  for 22 fine soils, and  $\pm 0.078/0.098 \text{ W}\cdot\text{m}^{-1}\cdot\text{K}^{-1}$  for all 39 soils. That outcome falls into the “good/superior” category. When applied to three Standard Sands, the structures of WAM<sub>s</sub>-1 and WAM<sub>s</sub>-2 were identical because the quartz was the only soil mineral.

Consequently, the  $\lambda_{\text{est}}$  of both models followed the experimental data closely; their average *SDs* were in a good performance range. Essentially, the WAM<sub>s</sub>-1, WAM<sub>s</sub>-2, and deV-1 models offered similar *SD* data ( $SD < 0.14 \text{ W}\cdot\text{m}^{-1}\cdot\text{K}^{-1}$ ) and their thermal conductivity trends closely followed experimental data.

When the models were applied to the thermal conductivity database of 10 Chinese soils, good  $\lambda_{\text{est}}$  were obtained with the deV-1 model, while both WAM<sub>s</sub> (without latent heat) provided only satisfactory thermal conductivity estimates. For four coarse soils (S-Ren: 001–002–003–011), the deV-1 model (with the apparent thermal conductivity of humid soil air) provided closer  $\lambda_{\text{est}}$  than WAM<sub>s</sub>-1 and WAM<sub>s</sub>-2 (without latent heat transfer). In contrast, for six fine soils (S-Ren: 004–005–006–007–008–009) WAM<sub>s</sub>-1 provided comparable  $\lambda_{\text{est}}$  value to deV-1. In general, both WAM<sub>s</sub> models underestimated the experimental data; therefore, additional model improvement by applying  $\lambda_{\text{a-app}}$  should perhaps be considered. Consequently, further investigations are needed to include the apparent thermal conductivity of humid soil air.

## 5 Conclusions and Recommendations

Two innovative weighted average models (WAM<sub>s</sub>-1 and WAM<sub>s</sub>-2) were developed, calibrated, and successfully verified using thermal conductivity data of 39 Canadian Field Soils and three, differently compacted, pure quartz sands (Standard Sands). The *SD* data, for 39 Canadian Field Soils, confirm that WAM<sub>s</sub>-1 produced better  $\lambda_{\text{est}}$  than WAM<sub>s</sub>-2. This outcome was likely due to a more realistic representation of the solid phase (*qtz/o-min*) in WAM<sub>s</sub>-1 by highlighting quartz as the most unique and dominant soil mineral. However, at soil dryness, both models, with some exceptions, generally underestimate the experimental data. In turn, the WAM<sub>s</sub>-2 offers outstanding simplicity, i.e., the simple structure of model, the least number of adjustable parameters, and easy tractability, while maintaining a good/superior  $\lambda_{\text{est}}$ . However, its representation of the soil solid phase does not fully reflect the dominant role of quartz, in terms of  $\theta_{\text{qtz}}$  and  $\lambda_{\text{qtz}}$ . Consequently, its estimates of thermal conductivity were slightly poorer for coarse sands.

In short, the overall predictive performance (*SD*) of all three models (WAM<sub>s</sub>-1, WAM<sub>s</sub>-2, and deV-1) falls into the superior category, i.e.,  $SD < 0.1 \text{ W}\cdot\text{m}^{-1}\cdot\text{K}^{-1}$ , for fine soils. Despite the superior/good  $\lambda_{\text{est}}$  by the three models, future work on modeling soil should be continued to further improve  $\lambda$  estimations, especially for coarse soils.

When the three models were applied to Standard Sands, the obtained  $\lambda_{\text{est}}$  followed the experimental data closely; their average *SDs* were in a good performance range ( $SD < 0.14 \text{ W}\cdot\text{m}^{-1}\cdot\text{K}^{-1}$ ) and their thermal conductivity trends closely followed experimental data.

When the three models were applied to the thermal conductivity database of 10 Chinese soils of unknown mineralogy, good  $\lambda_{\text{est}}$  were obtained with the deV-1 model (with apparent thermal conductivity of humid soil air), while both  $\text{WAM}_s$  (without latent heat) provided only satisfactory/acceptable estimates. In general, both  $\text{WAM}_s$  models underestimated the experimental data; therefore, additional model improvement by applying  $\lambda_{\text{a-app}}$  should perhaps be considered.

**Author Contributions** All authors contributed equally to the paper.

**Funding** Open access funding provided by Università degli Studi di Roma Tor Vergata within the CRUI-CARE Agreement. The authors received no financial support for the research, authorship, and/or publication of this article.

**Data Availability** The data used in this paper can be requested from the corresponding author.

## Declarations

**Conflict of interest** I declare that the authors have no competing interests as defined by Springer, or other interests that might be perceived to influence the results and/or discussion reported in this paper.

**Open Access** This article is licensed under a Creative Commons Attribution 4.0 International License, which permits use, sharing, adaptation, distribution and reproduction in any medium or format, as long as you give appropriate credit to the original author(s) and the source, provide a link to the Creative Commons licence, and indicate if changes were made. The images or other third party material in this article are included in the article's Creative Commons licence, unless indicated otherwise in a credit line to the material. If material is not included in the article's Creative Commons licence and your intended use is not permitted by statutory regulation or exceeds the permitted use, you will need to obtain permission directly from the copyright holder. To view a copy of this licence, visit <http://creativecommons.org/licenses/by/4.0/>.

## References

1. G. Bovesecchi, P. Coppa, S. Pistacchio, *Rev. Sci. Instrum.* (2018). <https://doi.org/10.1063/1.5019776>
2. M.L. McCombie, V.R. Tarnawski, G. Bovesecchi, P. Coppa, W.H. Leong, *Int. J. Thermophys.* (2017). <https://doi.org/10.1007/s10765-016-2161-y>
3. G. Bovesecchi, P. Coppa, *Int. J. Thermophys.* (2013). <https://doi.org/10.1007/s10765-01315032>
4. G. Bovesecchi, P. Coppa, M. Potenza, *Int. J. Thermophys.* (2017). <https://doi.org/10.1007/s10765-017-2202-1>
5. M. S. Kersten, *Thermal Properties of Soils*. Bulletin No. 28 (University of Minnesota, Minneapolis, USA, 1949) <https://hdl.handle.net/11299/124271>. Accessed 10 June 2022
6. D.A. de Vries, *Thermal Properties of Soils* (North-Holland Publishing Co., Amsterdam, 1963), pp.210–235
7. O. Johansen, *Thermal Conductivity of Soils*. Ph.D. Thesis, (University of Trondheim, Norway, 1975) <https://apps.dtic.mil/sti/citations/ADA044002>. Accessed 10 June 2022
8. G.S. Campbell, *Soil Physics with BASIC*. Transport Models for Soil-Plant Systems. (Elsevier Science Publishing Company, New York 1985)

9. G.S. Campbell, J.D. Jungbauer, W.R. Bidlake, R.D. Hungerford, *Soil Sci.* (1994). <https://doi.org/10.1097/00010694-199411000-00001>
10. F. Gori, *Int. Heat Transf. Conf.* (1986). <https://doi.org/10.1615/ihtc8.270>
11. B. Usowicz, Statistical-physical model of thermal conductivity in soil. (*Pol. J. Soil Sci.*, 1992) <http://users.ipan.lublin.pl/~usowicz/pdf/PJSS92.pdf> Accessed 10 June 2022
12. J. Côté, J.M. Konrad, *Can. Geotech. J.* (2005). <https://doi.org/10.1139/t04-106>
13. S. Lu, T. Ren, Y. Gong, R. Horton, *Soil Sci. Soc. Am. J.* (2007). <https://doi.org/10.2136/sssaj2006.0041>
14. V.R. Tarnawski, W.H. Leong, *Int. J. Thermophys.* (2012). <https://doi.org/10.1007/s10765-012-1282-1>
15. V.R. Tarnawski W.H. Leong, *Int. J. Thermophys.* (2016) <https://doi.org/10.1007/s10765-015-2024-y>
16. Z. Tian, Y. Lu, R. Horton, T. Ren, *Eur. J. Soil. Sci.* (2016). <https://doi.org/10.1111/ejss.12366>
17. V.R. Tarnawski, M.L. McCombie, W.H. Leong, P. Coppa, G. Bovesecchi, *Int. J. Thermophys.* (2018). <https://doi.org/10.1007/s10765-017-2357-9>
18. V.R. Tarnawski, F. Tsuchiya, P. Coppa, G. Bovesecchi, *Int. J. Thermophys.* (2019). <https://doi.org/10.1007/s10765-018-2480-2>
19. V.R. Tarnawski, P. Coppa, W.H. Leong, M.L. McCombie, G. Bovesecchi, *Int. J. Therm. Sci.* (2020). <https://doi.org/10.1016/j.ijthermalsci.2020.106493>
20. V.R. Tarnawski, B. Wagner, W.H. Leong, M.L. McCombie P. Coppa, G. Bovesecchi, *Eur J Soil Sci* (2021) <https://doi.org/10.1111/ejss.13117>
21. O.T. Farouki, *Thermal Properties of Soils* (Trans Tech Pub, Rockport, MA, USA, 1986) <https://apps.dtic.mil/sti/pdfs/ADA111734.pdf>. Accessed 10 June 2022
22. J. C. Maxwell, *A Treatise on Electricity and Magnetism*, vol. 1, 3rd Ed, (Oxford Univ Press. 1904)
23. H. Fricke, *Phys. Rev.* (1924). <https://doi.org/10.1103/PhysRev.24.575>
24. H. C. Burger, *Phys. Zs*, 20, (1915)
25. A. Eucken, *Ceram. Abstr.*, 11, (1932)
26. D.A. de Vries, *Nature* (1952). <https://doi.org/10.1038/1781074a0>
27. V.R. Tarnawski, T. Momose, M.L. McCombie, W.H. Leong, *Int. J. Thermophys.* (2015). <https://doi.org/10.1007/s10765-014-1793z>
28. V.R. Tarnawski, T. Momose, W.H. Leong, G. Bovesecchi, P. Coppa, *Int. J. Thermophys.* (2009). <https://doi.org/10.1007/s10765-009-0596-0>
29. V.R. Tarnawski, M.L. McCombie, T. Momose, I. Sakaguchi, W.H. Leong, *Int. J. Thermophys.* (2013). <https://doi.org/10.1007/s10765-0131455-6>
30. V.R. Tarnawski, T. Momose, W.H. Leong, *Géotechnique* (2009). <https://doi.org/10.1680/geot.2009.59.4.331>

**Publisher's Note** Springer Nature remains neutral with regard to jurisdictional claims in published maps and institutional affiliations.